Table S1. Primers Used to Prepare ToMOH Variants.

Variant	Primer
I100W	5’-CAA CTT CAC TTC GGA GCG TGG GCA CTT GAA GAA TAC G-3’
	5’-C GTA TTC TTC AAG TGC CCA CGC TCC GAA GTG AAG TTG-3’
I100A	5’-CAC TTC GGA GCG GCT GCA CTT GAA GAA TAC-3’
	5’-GTA TTC TTC AAG TGC AGC CGC TCC GAA GTG-3’
W167E	5’-CAT ACT AAC GAA GAA GCC GCA ATC GCG GCA CGG-3’
	5’-CCG TGC CGC GAT TGC GGC TTC TTC GTT AGT ATG-3’
F176A	5’-GCT GCA CGG TCT TTC GCT GAC GAC ATG ATG-3’
	5’-CAT CAT GTC GTC AGC GAA AGA CCG TGC AGC-3’
F176W	5’-GCA CGG TCT TTC TGG GAC GAC ATG ATG ATG -3’
	5’-CAT CAT CAT GTC GTC CCA GAA AGA CCG TGC -3’
F205A	5’-C AGC AAT ATG CAG GCT CTC GGT TTG GCC G-3’
	5’-C GGC CAA ACC GAG AGC CTG CAT ATT GCT G-3’
F205W	5’-GGC TTC AGC AAT ATG CAG TGG CTC GG T TTG GCC GCT GAC-3’
	5’- GTC AGC GGC CAA ACC GAG CCA CTG CAT ATT GCT GAA GCC-3’
L208W	5’-CAG TTT CTC GGT TGG GCC GCT GAC GCT G-3’
	5’-C AGC GTC AGC GGC CCA ACC GAG AAA CTG-3’
L208W/D211W	5’-G TTT CTC GGT TGG GCC GCT TGG GCT GCT G-3’
	5’-C AGC AGC CCA AGC GGC CCA ACC GAG AAA C-3’
V271A	5’-G AAG CTT TTC TCG GCT CTC ACC GGC CC-3’
	5’-GG GCC GGT GAG AGC CGA GAA AAG CTT C-3’
L272A	5’-G CTT TTC TCG GTA GCT ACC GGC CCC ATC-3’

	5’-GAT GGG GCC GGT AGC TAC CGA GAA AAG C-3’
L272E	5’-G CTT TTC TCG GTA GAA ACC GGC CCC ATC-3’
	5’-GAT GGG GCC GGT TTC TAC CGA GAA AAG C-3’
I276E	5’-GTA CTC ACC GGC CCC GAA ATG GAT TAT TAC AC-3’
	5’-GT GTA ATA ATC CAT TTC GGG GCC GGT GAG TAC-3’

Table S2. Fe Content and Specific Steady State Activity of ToMOH Variants.[a]

Variant	Location of the mutation	Fe Content, [Fe]/[ToMOH]	Specific steady state activity (mU/mg)	Relative steady state activity (%)[b]
Wild-type	-	3.7 ± 0.6	1200 ± 200	50 ± 10
T201S	-	4.15 ± 0.04	2400 ± 300	100
T201S/I100A	Cavity 1	4.14 ± 0.06	470 ± 130	20 ± 6
T201S/I100W	Cavity 1	3.43 ± 0.03	nd[d]	nd[d]
T201S/W167E	Cavity 3	5.97 ± 0.29[c]	720 ± 50	30 ± 4
T201S/F176A	Cavity 1	2.72 ± 0.10	1290 ± 80	54 ± 8
T201S/F176W	Cavity 1	3.19 ± 0.14	nd[d]	nd[d]
T201S/F205A	Cavity 1	2.76 ± 0.08	230 ± 50	10 ± 2
T201S/F205W	Cavity 1	4.72 ± 0.13	nd[d]	nd[d]
T201S/L208W	Channel	4.74 ± 0.09	nd[d]	nd[d]
T201S/L208W/D211W	Channel	4.10 ± 0.06	nd[d]	nd[d]
T201S/V271A	Cavity 2	3.22 ± 0.07	1140 ± 100	48 ± 7
T201S/L272A	Cavity 2	4.78 ± 0.02	940 ± 140	39 ± 8
T201S/L272E	Cavity 2	6.8 ± 0.1[c]	310 ± 40	13 ± 2
T201S/I276E	Channel	5.9 ± 0.1[c]	1400 ± 490	58 ± 22

[a]Fe content and specific steady state activity were measured in triplicate and the average and standard deviations were calculated. [b]Relative steady state activity of the variants were measured relative to the value of T201S single variant. The errors for the relative steady state activity are determined by propagating the standard deviation values for the variants. [c]A few variants contained > 4 Fe atoms per protein, possibly due to binding of adventitious iron. In such cases, the protein was reduced with dithionite and dialyzed anaerobically to remove the excess iron, which led to approximately 4 Fe ions per protein. [d]Not detected.

Table S3. X-ray Data Collection and Refinement Statistics for ToMOH Variants.

	T201S/I100A	T201S/I100W	T201S/W167E	T201S/F176W	T201S/V271A	T201S/L272E	T201S/I276E
Data Collection							
Beamline	NE-CAT 24 ID-E	NE-CAT 24 ID-E	NE-CAT 24 ID-E	NE-CAT 24 ID-E	SSRL 12-2	NE-CAT 24 ID-E	NE-CAT 24 ID-E
Wavelength (Å)	0.979	0.979	0.979	0.979	1.034	0.979	0.979
Space group	$P3_121$	$P3_121$	$P3_121$	$P3_121$	$P3_121$	$P3_121$	$P3_121$
Unit cell dimensions (Å)	182.6 x 182.6 x 67.0	182.8 x 182.8 x 67.7	182.6 x 182.6 x 68.3	183.1 x 183.1 x 68.0	183.4 x 183.4 x 68.3	182.4 x 182.4 x 67.5	183.0 x 183.0 x 68.0
Resolution range (Å)	30.0 - 2.75	50.0 – 3.00	50.0 – 2.80	50.0 – 2.65	50.0 – 2.2	50.0 – 2.80	50.0 – 2.50
Total reflections	195303	149031	199829	230251	598335	244050	293744
Unique reflections	27980	24140	29390	36462	66756	30252	43135
Completeness (%)[a]	93.7 (95.3)	96.6 (97.4)	96.6 (97.9)	99.7 (100)	99.7 (100)	99.6 (100)	99.7 (99.8)
$I/\sigma(I)$[a]	21.8 (4.0)	30.1 (9.0)	26.2 (4.6)	33.1 (7.4)	16.4 (6.9)	25.3 (7.2)	26.9 (5.2)
R_{sym} (%)[a,b]	10.2 (42.1)	10.3 (26)	10.1 (42.3)	9.2 (36.6)	10.0 (31.7)	13.9 (40.8)	9.9 (39.3)
Refinement							
R_{cryst} (%)[c]	19.0	18.0	19.5	17.8	15.6	16.4	18.4

R_{free} (%)[d]	25.1	24.1	26.0	23.5	20.0	22.7	23.4
Average B-value ($Å^2$)	64.1	53.0	52.3	45.9	24.2	27.6	42.8
r.m.s deviation bond length (Å)	0.008	0.016	0.015	0.019	0.024	0.016	0.021
r.m.s deviation bond angles (°)	1.11	1.65	1.66	1.81	1.81	1.61	1.83
No. protein atoms	7331	7340	7329	7368	7355	7348	7335
No. non-protein atoms	53	57	51	169	586	239	298
Fe atoms	2	2	2	2	2	2	2
Water molecules	46	55	49	152	566	212	296
PEG-400 fragments[e]	1	0	0	0	2	2	0
RMSD to wild-type ToMOH	0.20	0.19	0.23	0.16	0.17	0.16	0.15
PDB Code	3RNC	3RNA	3RNG	3RNB	3RNF	3RN9	3RNE

[a]Values in parentheses are for the highest resolution shell. [b]$R_{sym} = \Sigma_i\Sigma_{hkl}|I_i(hkl) - \langle I(hkl)\rangle| / \Sigma_{hkl}\langle I(hkl)\rangle$, where $I_i(hkl)$ is the *i*th measured diffraction intensity and $\langle I(hkl)\rangle$ is the mean intensity for the Miller index (*hkl*). [c]$R_{cryst} = \Sigma_{hkl}||F_o(hkl)| - |F_c(hkl)|| / \Sigma_{hkl}|F_o(hkl)|$. [d]$R_{free} = R_{cryst}$ for a test set of reflections (5% in each case). [e]A second PEG-400 molecule is observed in the T201S/V271A and T201S/L272E variants. They are positioned in the cavity 3 as shown in Fig S5.

Figures Captions

Figure S1. (A) Superposition of residues gating access between cavities 1 and 2 in T4moH-T4moD (green sticks) and ToMOH (blue sticks) structures. Cavity 2 of the T4moH-T4moD structure is shown as red surfaces. Distances between L272 and L268, A172, and A99 in the T4moH-T4moD structure are 6.7 Å, 8.0 Å, and 4.5 Å, respectively. (B) Superposition of the T4moH-T4moD complex and ToMOH T201S/L272E (cyan sticks).

Figure S2. Plots of formation rate constants of $T201_{peroxo}$ vs dioxygen concentrations. Formation and decay rates were measured in the reaction of reduced ToMOH variants and ToMOD with various concentrations of dioxygen. Figures are arranged from top to bottom as: (A) T201S, (B) T201S/I100W, (C) T201S/L272E, (D) T201S/V271A, (E) T201S/W167E, and (F) T201S/I276E ToMOH variants. Formation and decay rate constants are represented as black squares and red circles, respectively. Both formation and decay rates were fit to a linear function as depicted with black and red lines, respectively. Second-order formation rate constants were obtained from the slope of a linear fit. Linear fits of decay rates in all variants, shown in red, yielded zero or very small slopes indicating that decay of $T201_{peroxo}$ is independent of O_2 concentration.

Figure S3. Structural changes in the T201S/F176W ToMOH variant. The F176W substitution contracts the entrance to cavity 1. The closest C···C distance between the I100 and F176 is 6.0 Å in the T201S variant is reduced to 4.2 Å by the F176W mutation.

Figure S4. Structural changes in the T201S/W167E ToMOH variant. (A) Change in distances between W167E and nearby residues between cavities 2 and 3. Wild-type and W167E ToMOH gating residues are depicted as gray and green sticks, respectively. The distance between the W167E δ1 oxygen and V271 γ carbon atoms is 7.8 Å (not shown). (B) Newly formed hydrogen bonds between W167E and adjacent residues, E166 and T341. Oxygen and nitrogen atoms in W167E, E166, and T341 residues are depicted by red and blue sticks, respectively.

Figure S5. A second PEG 400 molecule, in addition to one observed in the channel of the wild-type and T201S/I100A proteins, is observed in cavity 3 of the (A) T201S/L272E and (B) T201S/V271A ToMOH variants. In (A) the cavity 3 surfaces are colored light yellow and a $2F_o$-F_c omit map for PEG is contoured to 1.0 σ (blue mesh). Residues delineating the gate between cavities 2 and 3 are represented by green sticks. The oxygen and carbon atoms of PEG are depicted by red and gray sticks, respectively. Ribbon structures at the top right of the panel correspond to the ToMOH γ-subunit. In (B), cavity surfaces are depicted pink as in Fig 2D to denote connectivity between all three cavities. Atoms and molecules are depicted as in (A), with the exception of the γ-subunit, which is not shown.

Figure S1.

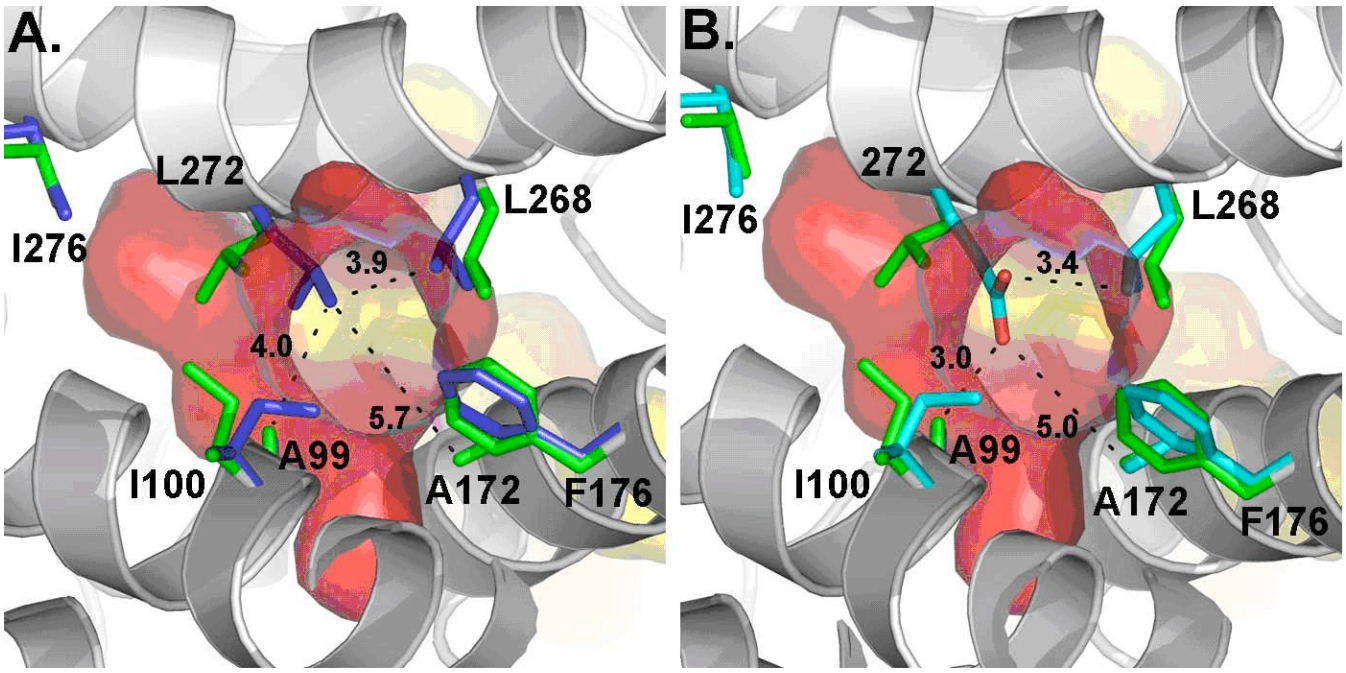
A.
L272
L268
I276
3.9
4.0
5.7
A99
I100
A172
F176
B.
272
I276
L268
3.4
3.0
5.0
A99
I100
A172
F176

Figure S2A.

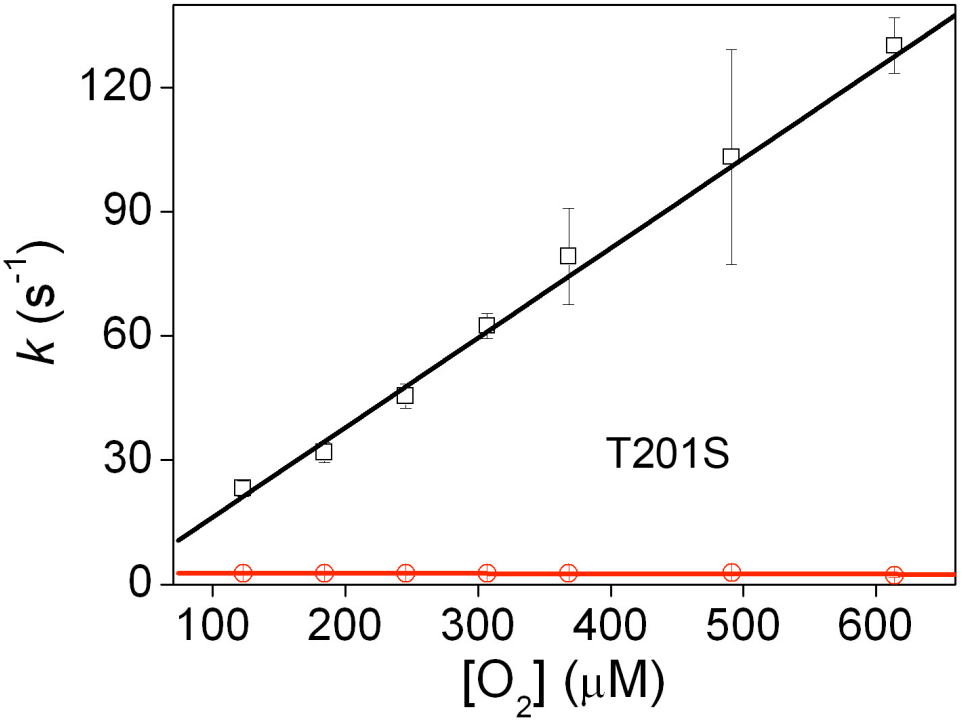

Figure S2B.

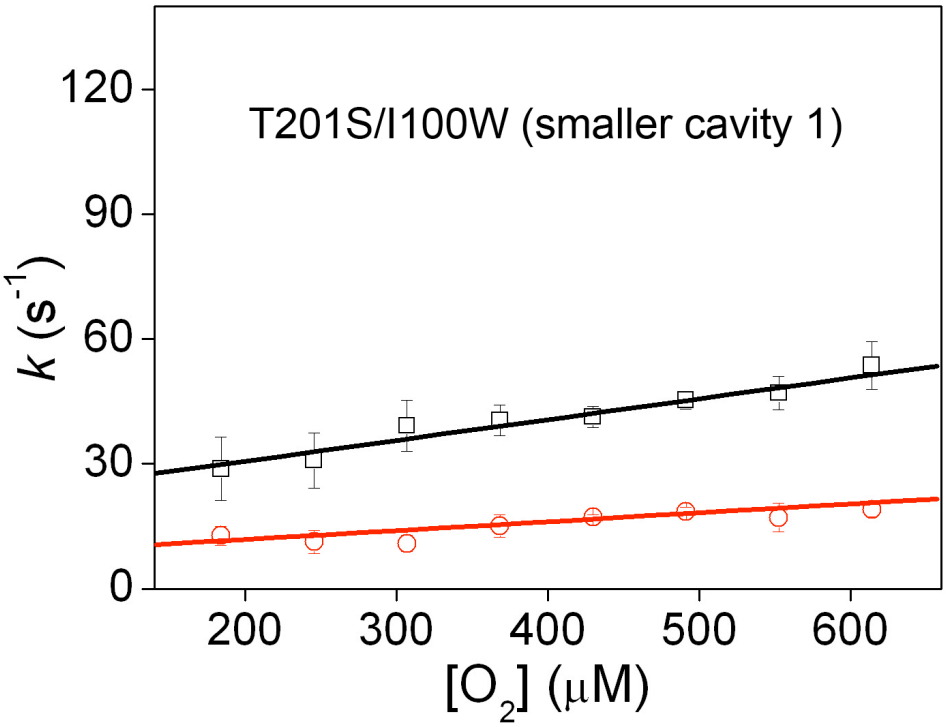

Figure S2C.

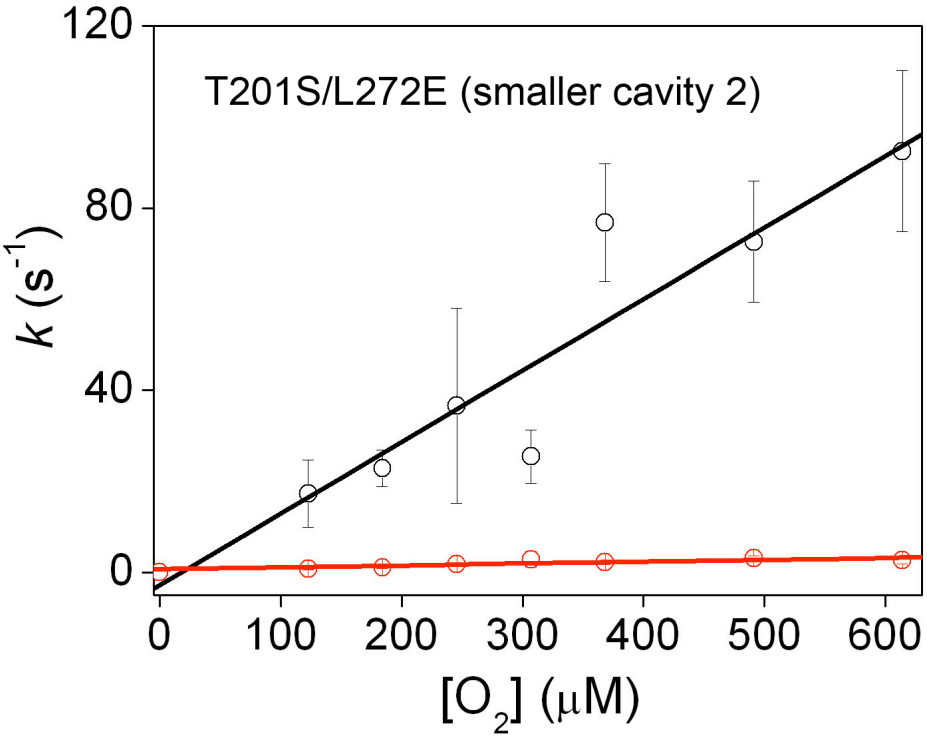

Figure S2D.

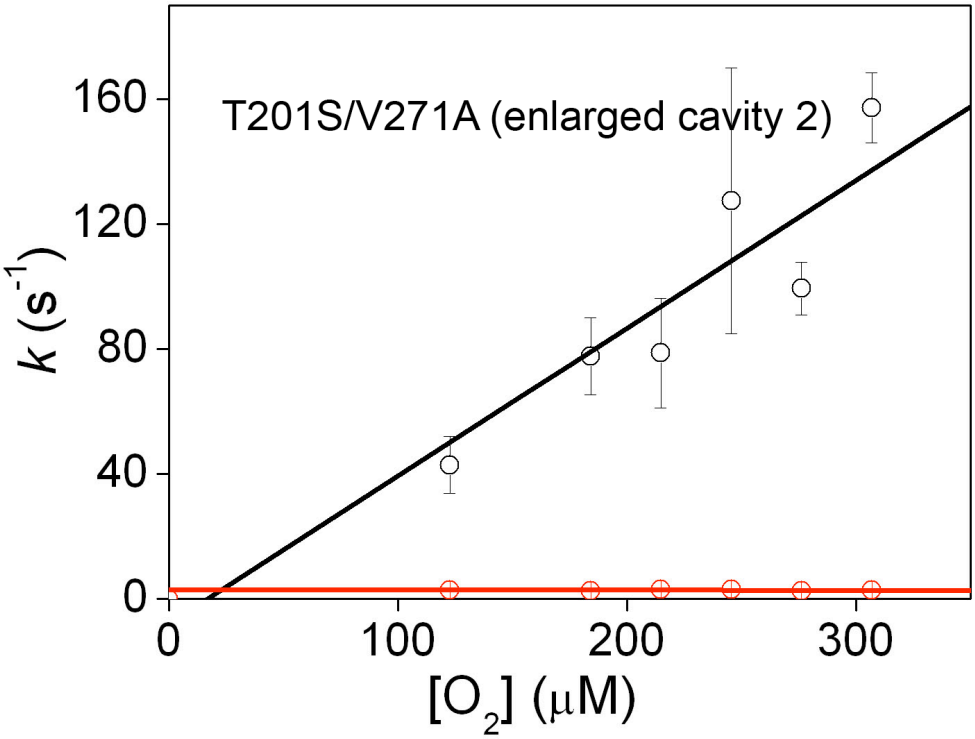

Figure S2E.

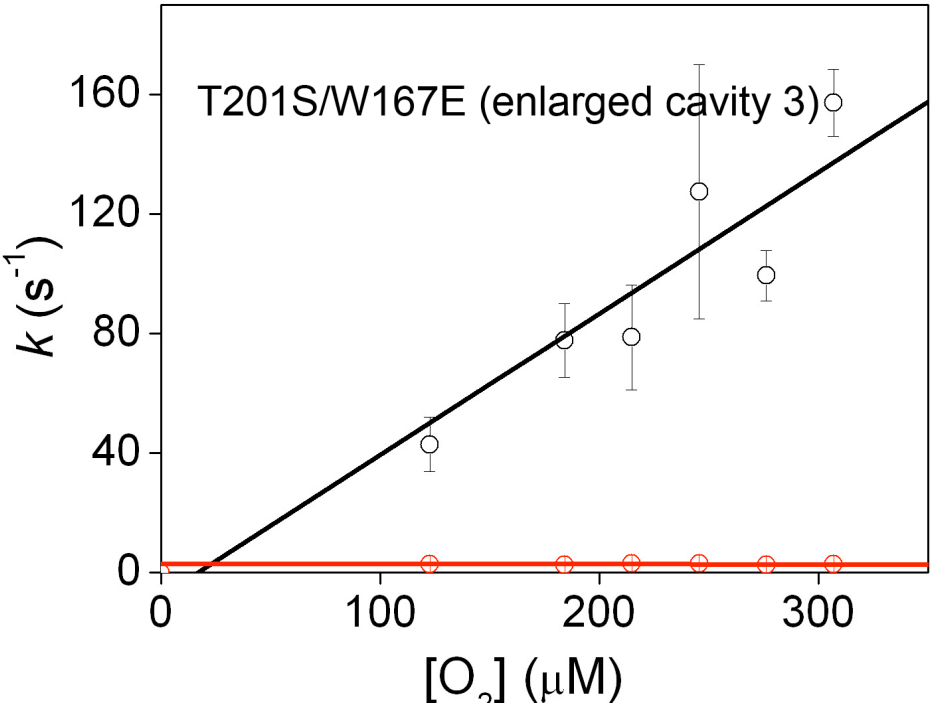

Figure S2F.

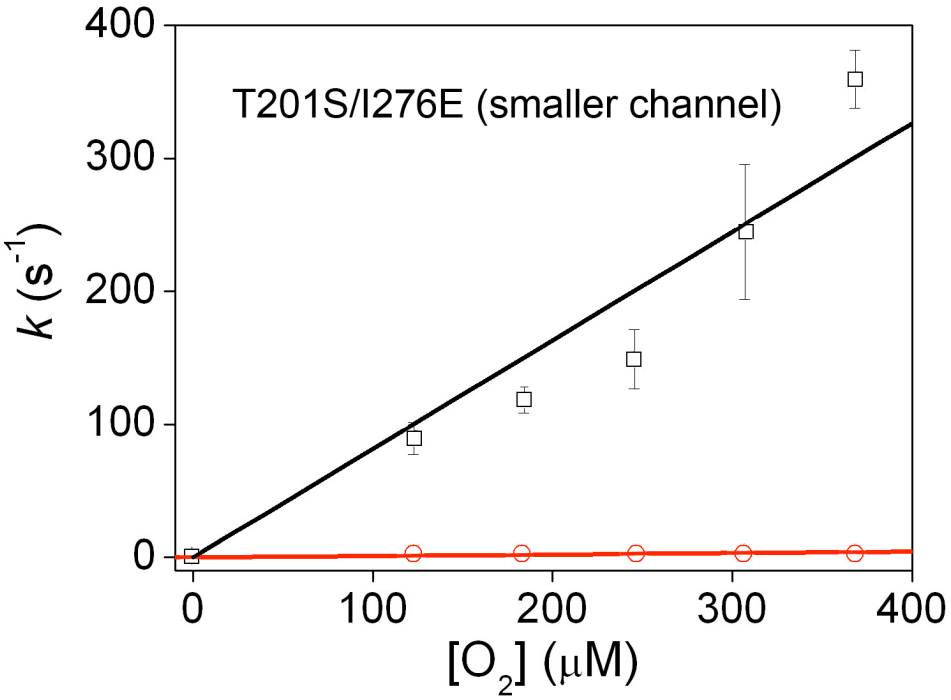

Figure S3.

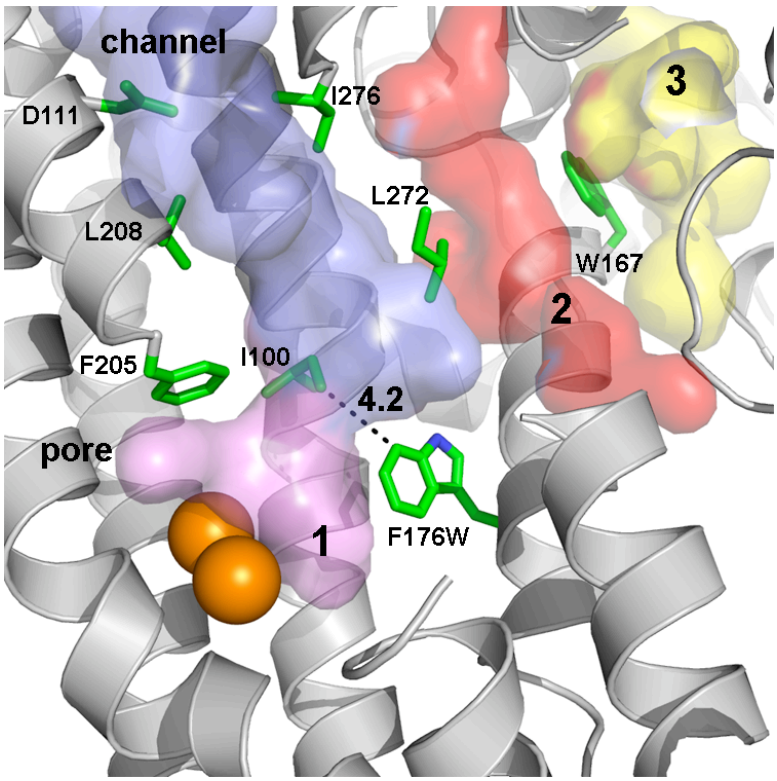

Figure S4.

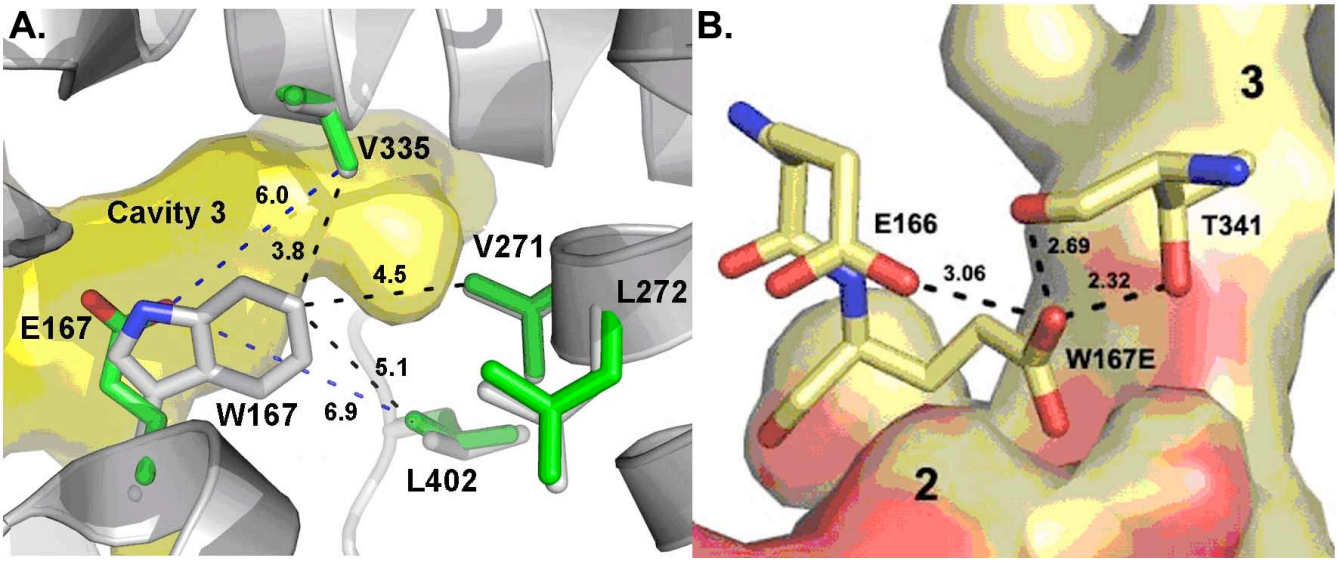

Figure S5.